Central Washington University

ScholarWorks@CWU

12-18-2015

Characterizing Far-infrared Laser Emissions and the Measurement of Their Frequencies

Michael Jackson

Lyndon R. Zink

Video Article

Characterizing Far-infrared Laser Emissions and the Measurement of Their Frequencies

Michael Jackson[1,3], Lyndon R. Zink[2]

[1]Department of Physics, Central Washington University

[2]Department of Physics, University of Wisconsin-La Crosse

[3]College of Science and Technology, Millersville University

Correspondence to: Michael Jackson at mjackson@millersville.edu

Abstract

The generation and subsequent measurement of far-infrared radiation has found numerous applications in high-resolution spectroscopy, radio astronomy, and Terahertz imaging. For about 45 years, the generation of coherent, far-infrared radiation has been accomplished using the optically pumped molecular laser. Once far-infrared laser radiation is detected, the frequencies of these laser emissions are measured using a three-laser heterodyne technique. With this technique, the unknown frequency from the optically pumped molecular laser is mixed with the difference frequency between two stabilized, infrared reference frequencies. These reference frequencies are generated by independent carbon dioxide lasers, each stabilized using the fluorescence signal from an external, low pressure reference cell. The resulting beat between the known and unknown laser frequencies is monitored by a metal-insulator-metal point contact diode detector whose output is observed on a spectrum analyzer. The beat frequency between these laser emissions is subsequently measured and combined with the known reference frequencies to extrapolate the unknown far-infrared laser frequency. The resulting one-sigma fractional uncertainty for laser frequencies measured with this technique is ± 5 parts in 10^7. Accurately determining the frequency of far-infrared laser emissions is critical as they are often used as a reference for other measurements, as in the high-resolution spectroscopic investigations of free radicals using laser magnetic resonance. As part of this investigation, difluoromethane, CH_2F_2, was used as the far-infrared laser medium. In all, eight far-infrared laser frequencies were measured for the first time with frequencies ranging from 0.359 to 1.273 THz. Three of these laser emissions were discovered during this investigation and are reported with their optimal operating pressure, polarization with respect to the CO_2 pump laser, and strength.

Video Link

The video component of this article can be found at http://www.jove.com/video/53399/

Introduction

The measurement of far-infrared laser frequencies was first performed by Hocker and co-workers in 1967. They measured the frequencies for the 311 and 337 µm emissions from the direct-discharge hydrogen cyanide laser by mixing them with high order harmonics of a microwave signal in a silicon diode[1]. To measure higher frequencies, a chain of lasers and harmonic mixing devices were used to generate the laser harmonics[2]. Eventually two stabilized carbon dioxide (CO_2) lasers were chosen to synthesize the necessary difference frequencies[3,4]. Today, far-infrared laser frequencies up to 4 THz can be measured with this technique using only the first harmonic of the difference frequency generated by two stabilized CO_2 reference lasers. Higher frequency laser emissions can also be measured using the second harmonic, such as the 9 THz laser emissions from the methanol isotopologues CHD_2OH and $CH_3^{18}OH$.[5,6] Over the years, the accurate measurement of laser frequencies has impacted a number of scientific experiments[7,8] and permitted the adoption of a new definition of the meter by the General Conference of Weights and Measures in Paris in 1983.[9–11]

Heterodyne techniques, such as those described, have been immensely beneficial in the measurement of far-infrared laser frequencies generated by optically pumped molecular lasers. Since the discovery of the optically pumped molecular laser by Chang and Bridges[12], thousands of optically pumped far-infrared laser emissions have been generated with a variety of laser media. For example, difluoromethane (CH_2F_2) and its isotopologues generate over 250 laser emissions when optically pumped by a CO_2 laser. Their wavelengths range from approximately 95.6 to 1714.1 µm.[13–15] Nearly 75% of these laser emissions have had their frequencies measured while several have been spectroscopically assigned[16–18].

These lasers, and their accurately measured frequencies, have played a crucial role in the advancement of high-resolution spectroscopy. They provide important information for infrared spectral studies of the laser gases. Often these laser frequencies are used to verify the analysis of infrared and far-infrared spectra because they provide connections among the excited vibrational state levels that are often directly inaccessible from absorption spectra[19]. They also serve as the primary radiation source for studies investigating transient, short-lived free radicals with the laser magnetic resonance technique[20]. With this extremely sensitive technique, rotational and ro-vibrational Zeeman spectra in paramagnetic

atoms, molecules, and molecular ions can be recorded and analyzed along with the ability to investigate the reaction rates used to create these free radicals.

In this work, an optically pumped molecular laser, shown in **Figure 1**, has been used to generate far-infrared laser radiation from difluoromethane. This system consists of a continuous wave (cw) CO_2 pump laser and a far-infrared laser cavity. A mirror internal to the far-infrared laser cavity redirects the CO_2 laser radiation down the polished copper tube, undergoing twenty six reflections before terminating at the end of the cavity, scattering any remaining pump radiation. Therefore the far-infrared laser medium is excited using a transverse pumping geometry. To generate laser action, several variables are adjusted, some simultaneously, and all are subsequently optimized once laser radiation is observed.

In this experiment, far-infrared laser radiation is monitored by a metal-insulator-metal (MIM) point contact diode detector. The MIM diode detector has been used for laser frequency measurements since 1969.[21–23] In laser frequency measurements, the MIM diode detector is a harmonic mixer between two or more radiation sources incident on the diode. The MIM diode detector consists of a sharpened Tungsten wire contacting an optically polished Nickel base[24]. The Nickel base has a naturally occurring thin oxide layer that is the insulating layer.

Once a laser emission was detected, its wavelength, polarization, strength, and optimized operating pressure were recorded while its frequency was measured using the three-laser heterodyne technique[25–27] following the method originally described in Ref. 4. **Figure 2** shows the optically pumped molecular laser with two additional cw CO_2 reference lasers having independent frequency stabilization systems that utilize the Lamb dip in the 4.3 µm fluorescence signal from an external, low pressure reference cell[28]. This manuscript outlines the process used to search for far-infrared laser emissions as well as the method for estimating their wavelength and in accurately determining their frequency. Specifics regarding the three-laser heterodyne technique as well as the various components and operating parameters of the system can be found in Supplemental Table A along with references 4, 25–27, 29, and 30.

Protocol

1. Planning of Experiments

1. Conduct a survey of the literature to assess prior work performed using the laser medium of interest, which for this experiment is CH_2F_2. Identify all known laser emissions along with all information about the lines such as their wavelength and frequency. Several surveys of known laser emissions are available[13,31–37].
2. Compile all spectroscopic investigations of the molecule used as the laser medium with a focus on prior Fourier transform[34] and optoacoustic studies[38,39].

2. Generating Far-Infrared Laser Emissions

1. Safety Overview.
   1. Develop a standard operating procedure for the lab that includes proper eye protection when working with the CO_2 and far-infrared laser systems.

2. Alignment and Calibration.
   1. Calibrate each CO_2 laser using a grating-based spectrum analyzer designed for the CO_2 laser according to the manufacturer's protocol.
   2. Align the end mirrors and the coupling mirror in the far-infrared laser cavity using a He-Ne laser so that their radiation is focused onto the MIM diode detector.
   3. Direct the radiation from the CO_2 pump laser into the far-infrared laser cavity through a sodium chloride window at an angle of approximately 72° with respect to the cavity axis.
   4. Direct the radiation from the two CO_2 reference lasers to either their respective low-pressure fluorescence reference cell or co-linearly onto the MIM diode detector using beam splitters and additional mirrors.

3. Detection of far-infrared laser radiation.
   1. Polish the Nickel base every several days using a standard metal polish.
   2. Crimp a 25 µm tungsten wire into a copper post and bend the wire into the configuration shown in **Figure 3**.
   3. Adjust the length of the wire so that it is between 10 to 20 wavelengths of the radiation being measured.
   4. Electrochemically etch the tip of the wire in a saturated sodium hydroxide (NaOH) solution by applying a voltage (approximately 3.5 to 5 VAC) to the solution.
   5. Re-etch the tip with a low voltage (less than 1 VAC). This roughens the tip of the wire and improves the diode's performance.
   6. Rinse the wire with distilled water.
   7. Insert the copper post into the MIM diode's housing once the wire is dry.
   8. Place the wire in contact with the Nickel base using a fine screw and level system. Contacts yielding a resistance across the diode between 100 and 500 Ω are typically used when detecting and measuring far-infrared laser radiation.

4. Generation of far-infrared laser radiation.
   1. Set the CO_2 pump laser on a specific laser emission, *e.g.*, 9*P*36.
   2. Rotate the micrometer dial on the CO_2 pump laser back and forth to achieve maximum intensity on the beam stop.
   3. Adjust the tilt of the CO_2 pump laser's grating to achieve maximum intensity on the beam stop.
   4. Repeat steps 2.4.2 and 2.4.3 until the output power for the CO_2 pump laser appears optimized on the beam stop.
   5. Remove the beam stop from the path of the CO_2 pump laser.
   6. Turn on and align the optical chopper into the beam path of the CO_2 pump laser.

7. Open the valve on the CH_2F_2 cylinder to introduce the far-infrared laser medium into the far-infrared laser cavity.
8. Adjust the metering valve on the inlet line until a pressure of approximately 10 Pa is achieved.
   Note: Only the approximate pressure is necessary since it is used as a way of systematically scanning the far-infrared laser cavity.
9. Set the position of the output coupler such that its outermost tip is approximately 1 cm from the middle of the laser cavity as indicated by a calibrated scale on the outside of the laser cavity.
   Note: Only the approximate location is necessary since it is used as a way of systematically scanning the far-infrared laser cavity.
10. Adjust the position of the moveable far-infrared laser mirror in approximately 0.25 mm increments by rotating the calibrated micrometer dial back and forth. Simultaneously tune the frequency of the CO_2 pump laser through its gain curve by changing the voltage applied across the CO_2 pump laser's piezoelectric transducer (PZT).
11. If no signal is observed on the oscilloscope display, repeat step 2.4.10 with the output coupler moved to its next position where the tip is approximately 1.5 cm from the middle of the laser cavity as indicated by a calibrated scale on the outside of the laser cavity.
12. If no signal is observed on the oscilloscope display, repeat step 2.4.10 with the output coupler moved to its next position where the tip is approximately 2 cm from the middle of the laser cavity as indicated by a calibrated scale on the outside of the laser cavity.
13. If no signal is observed on the oscilloscope display, repeat steps 2.4.9 through 2.4.12 with a far-infrared laser pressure of approximately 19 Pa as adjusted with the metering valve on the inlet line.
14. If no signal is observed on the oscilloscope display, repeat steps 2.4.9 through 2.4.12 with a far-infrared laser pressure of approximately 27 Pa as adjusted with the metering valve on the inlet line.
15. If no signal is observed on the oscilloscope display, insert the beam stop into the path of the CO_2 pump laser and close the valve on the CH_2F_2 cylinder until the far-infrared laser pressure is approximately 0 Pa.
16. Set the CO_2 pump laser to the next laser emission, *e.g.,* 9*P*34, and optimize the output power using steps 2.4.2 through 2.4.4.
17. Repeat steps 2.4.5 through 2.4.16 until all emissions generated by the CO_2 pump laser are used. When searching for far-infrared laser lines, place a focus on CO_2 pump laser emissions whose frequencies overlap with any absorption regions identified in step 1.2.

5. Characterizing far-infrared laser emissions.
   1. Simultaneously adjust the pressure of the far-infrared laser medium, the voltage applied to the CO_2 pump laser's PZT, and the position of the output coupler until the far-infrared laser emission's output power is maximized (determined by a maximum peak-to-peak signal from the MIM diode detector as observed on the oscilloscope display, similar to **Figure 4**).
   2. Turn the micrometer dial clockwise until the far-infrared laser emission is observed on the oscilloscope display. Record the position of the micrometer dial.
   3. Turn the micrometer dial clockwise for an additional 20 modes corresponding to the same far-infrared laser emission. Record the position of the micrometer dial.
   4. Subtract the position of the micrometer dial in steps 2.5.2 and 2.5.3. Divide this difference by 10 to obtain the wavelength of the far-infrared laser emission.
   5. Repeat steps 2.5.2 through 2.5.4 a total of five times and average the wavelength of the far-infrared laser emission. Average laser wavelengths measured by traversing at least 20 adjacent longitudinal modes have a one-sigma uncertainty of ± 0.5 μm.
   6. Measure the polarization of the far-infrared laser radiation, relative to the CO_2 pump radiation, using either a gold wire-grid polarizer (394 lines/cm) or a Brewster polarizer.

3. Determining Far-Infrared Laser Frequencies

1. Identifying the CO_2 reference laser emissions.
   1. Calculate the frequency of the far-infrared laser emission based on its measured wavelength.
   2. Identify sets of CO_2 reference laser lines whose frequency difference is within several GHz of the calculated frequency for the far-infrared laser emission[40]. A typical list used for such measurements is shown in **Table 1**.

2. Searching for the heterodyne beat signal.
   1. Identify the first set of CO_2 reference laser lines and set each CO_2 reference laser on their respective laser emission.
   2. Optimize the output power for each CO_2 reference laser using steps 2.4.2 through 2.4.4 and the monitor power meter.
      1. Adjust an iris, either internal or external to each reference laser, so that the power from each CO_2 reference laser is approximately 100 mW as measured by the monitor power meter shown in **Figure 2**.
   3. Block the radiation from the CO_2 pump laser using a beam stop while unblocking the radiation from the CO_2 reference lasers.
   4. Turn on and align the optical chopper into the co-linear beam path of the CO_2 reference lasers.
   5. Optimize for maximum peak-to-peak voltage each CO_2 reference laser emission on the MIM diode detector using several mirrors, beam splitters, and a 2.54 cm focal length ZnSe plano-convex lens while observing the output on the oscilloscope, similar to **Figure 5**.
   6. Block the radiation from the CO_2 reference lasers using a beam stop while unblocking the radiation from the CO_2 pump laser.
   7. Re-optimize the CO_2 pump laser and the far-infrared laser, as necessary, so that the far-infrared laser emission has a maximum peak-to-peak voltage as observed on the oscilloscope.
   8. Disconnect the MIM diode detector's output from the oscilloscope and connect it to an amplifier whose output is observed on a spectrum analyzer.
   9. Unblock the radiation from the CO_2 reference lasers.
   10. Remove the optical choppers modulating the CO_2 pump and reference lasers.
   11. Set the spectrum analyzer on a 40 MHz span and search for the beat signal in 1.5 GHz increments by manually scanning this frequency range using the spectrum analyzer's adjustment knob.
   12. If no beat signal is observed, disconnect the MIM diode's output from the amplifier and connect it to the oscilloscope.
   13. Block the radiation from the CO_2 reference lasers and reinsert the optical chopper into the path of the CO_2 pump laser.
   14. Repeat steps 3.2.2 through 3.2.13 as necessary until the spectrum analyzer has been used to search for the beat signal between 0 and 12 GHz.

15. If no beat signal is observed, repeat steps 3.2.2 through 3.2.14 with another set of CO_2 reference laser lines until either the beat signal is observed or all possible sets of CO_2 reference laser lines are exhausted.

3. Stabilizing the CO_2 reference frequencies.
    1. Apply a voltage between 0 and 900 V to the first CO_2 reference laser's PZT so that the signal from its respective fluorescence reference cell is at the center of the Lamb dip, illustrated in **Figure 6** and as viewed on an oscilloscope as in **Figure 7**.
    2. Activate the feedback voltage applied to the first CO_2 reference laser's PZT using a custom built lock-in/servo amplifier so that it remains locked to the center of the Lamb dip.
    3. Repeat steps 3.3.1 and 3.3.2 for the second CO_2 reference laser.
    4. Visually monitor the output of the pre-amp on an oscilloscope, as in **Figure 7**, to ensure the reference lasers remains locked.

4. Measurement of the beat frequency.
    1. Center the beat signal on the spectrum analyzer display and adjust its amplitude to maximize its size on the display.
    2. Set the spectrum analyzer to view two simultaneous traces of the beat signal, as in **Figure 8**, by selecting the Clear Write feature for both Trace 1 and Trace 2. One trace will display the instantaneous signal while the other will record the maximum signal (using a Max Hold feature on the spectrum analyzer for the second trace).
    3. Rotate the micrometer dial on the far-infrared laser cavity back and forth across the gain curve for a given cavity mode.
    4. Use the View feature on the spectrum analyzer to freeze the second (Max Hold) trace once a symmetric pattern is obtained.
    5. Slightly rotate the micrometer dial clockwise to decrease the length of the far-infrared laser cavity. Simultaneously observe the subsequent small shift in the beat frequency on the spectrum analyzer due to this slight increase in the frequency of the far-infrared laser.
    6. Place markers at the full width at half maximum points of the symmetric pattern (Max Hold trace) using the Marker function with the Delta feature on the spectrum analyzer.
    7. Measure the center frequency of the beat signal using the Span Pair feature on the spectrum analyzer.
    8. Repeat steps 3.4.1 through 3.4.7.
    9. Disengage the lock in/servo amplifier for each CO_2 reference laser to unlock each laser from its center frequency and re-optimize each CO_2 reference laser.
    10. Re-lock the reference lasers using steps 3.3.1 through 3.3.4.
    11. Repeat steps 3.4.1 through 3.4.10 for a total of 6 measurements. Once complete, unlock each CO_2 reference laser from its center frequency.
    12. Calculate the revised frequency of the far-infrared laser emission using these beat frequencies to obtain an accurate prediction for the second set of CO_2 reference laser lines.
    13. Identify a different set of CO_2 reference laser lines whose frequency difference is within several GHz of the calculated frequency for the far-infrared laser emission.
    14. Optimize the next set of CO_2 reference laser lines on the MIM diode detector and obtain the beat signal using steps 3.2.2 through 3.2.15 as necessary.
    15. Lock the new set of CO_2 reference laser lines using steps 3.3.1 through 3.3.4.
    16. Repeat steps 3.4.1 through 3.4.10 for a total of 6 measurements. Once complete, unlock each CO_2 reference laser from its center frequency.
    17. Insert beam stops into the paths of the CO_2 pump and reference lasers.

5. Calculation of the far-infrared laser frequency.
    1. Calculate the unknown far-infrared laser frequency, v_{FIR}, using the measured beat frequency through the relation

    $$FIR = |v_{CO2(I)} - v_{CO2(II)}| \pm |v_{beat}| \qquad \text{Eq. 1}$$

    where $|v_{CO2(I)} - v_{CO2(II)}|$ is the magnitude of the difference frequency synthesized by the two CO_2 reference lasers and $|v_{beat}|$ is the magnitude of the beat frequency. The ± sign in Eq. 1 is determined experimentally from step 3.4.5.
    2. Obtain an average frequency and calculate the uncertainty.

Representative Results

As mentioned, the frequency reported for a far-infrared laser emission is an average of at least twelve measurements performed with at least two different sets of CO_2 reference laser lines. **Table 2** outlines the data recorded for the 235.5 µm laser emission when using the 9P04 CO_2 pump laser. For this far-infrared laser emission, fourteen individual measurements of the beat frequency were recorded. The first set of measurements were recorded while using the 9R10 and 9P38 CO_2 reference laser emissions. For step 3.4.5, as the far-infrared laser frequency was increased slightly, the beat frequency was also observed to increase. This indicates the far-infrared laser frequency was greater than the magnitude of the difference frequency between the 9R10 and 9P38 CO_2 reference lasers, $|v_{CO2(I)} - v_{CO2(II)}|$. Therefore the sign of the beat frequency in Equation 1 was positive for this set of CO_2 reference lasers. Conversely, the second set of measurements used the 9R16 and 9P34 CO_2 reference laser emissions. When step 3.4.5 was performed, a decrease in the beat frequency was observed while the far-infrared laser frequency was increased slightly. This indicates the far-infrared laser frequency was less than the magnitude of the difference frequency between the 9R16 and 9P34 CO_2 reference lasers. Therefore, for this set of CO_2 reference lasers the sign of the beat frequency in Equation 1 was negative. As illustrated in **Table 2**, the calculated far-infrared laser frequency, v_{FIR}, for both situations remained the same to within a ± 0.12 MHz one-sigma standard deviation.

The average far-infrared laser frequencies determined with this experimental technique are listed in **Table 3** and are arranged in order of the CO_2 pump line. The average laser frequencies are reported with their corresponding wavelength and wavenumber, calculated using 1 cm^{-1} = 29 979.2458 MHz. All far-infrared laser frequencies were measured under optimal operating conditions. Throughout this investigation, several previously reported frequencies were measured and were found to be in agreement with the published values. The one-sigma fractional uncertainty, Δv, of far-infrared laser frequencies measured with this technique is ± 5 × 10^{-7}. This uncertainty is derived from the reproducibility

of known frequencies with this system, the symmetry and width of the broadened gain curve of the far-infrared laser, and the precision of the measurements[4,25,31].

The far-infrared laser emissions discovered during this investigation were observed to have a strength of 'W' corresponding to a range in power from 0.001 to 0.01 mW. For comparison, the 118.8 µm line of methanol was observed with this system to be VVS with a power slightly above 10 mW when using the 9P36 CO_2 pump having a power of 18 W. Additionally, **Table 3** includes the polarization of each new far-infrared laser emission measured relative to its respective CO_2 pump laser. In most cases, only one polarization was observed to dominate, either a polarization parallel or perpendicular to the CO_2 pump laser. For situations where no dominant polarization was observed, both polarizations have been listed.

In sum, eight far-infrared laser emissions were generated by difluoromethane using an optically pumped molecular laser system having a transverse pumping geometry. This includes the discovery of three far-infrared laser emissions having wavelengths of 235.5, 335.9, and 416.8 µm. Once detected, the three-laser heterodyne technique was used to measure the frequency for each observed far-infrared laser emission. The frequencies for these laser emissions ranged from 0.359 to 1.273 THz and are reported with fractional uncertainties of ± 5 parts in 10[7].
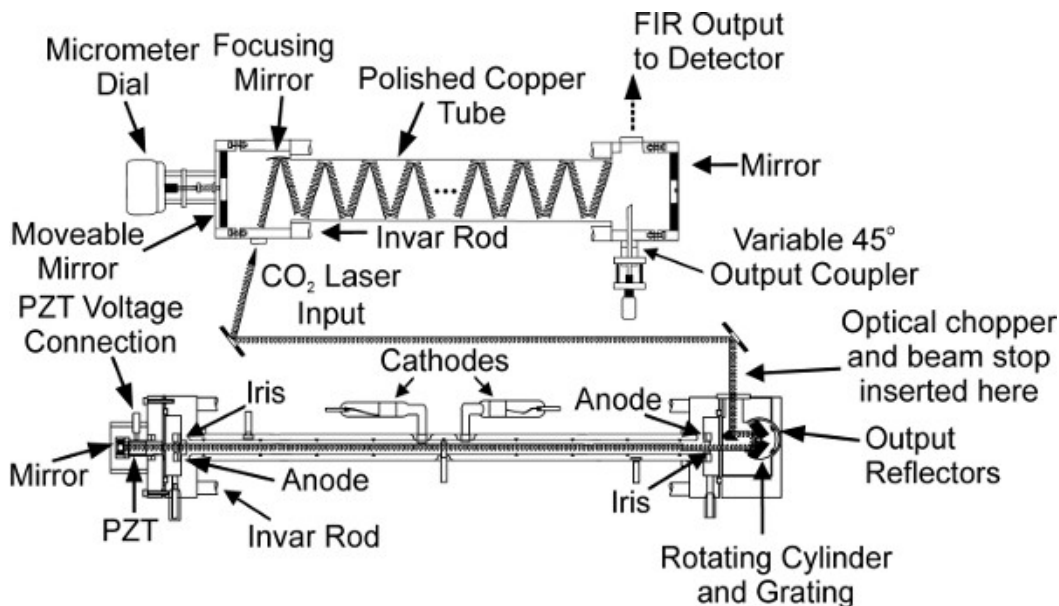

Figure 1. Schematic diagram of the optically pumped molecular laser system consisting of a carbon dioxide pump laser and a far-infrared laser cavity. The far-infrared laser medium is excited using a transverse pumping geometry. Reprinted with minor modifications from Ref. 15 with kind permission from Springer Science and Business Media. Please click here to view a larger version of this figure.
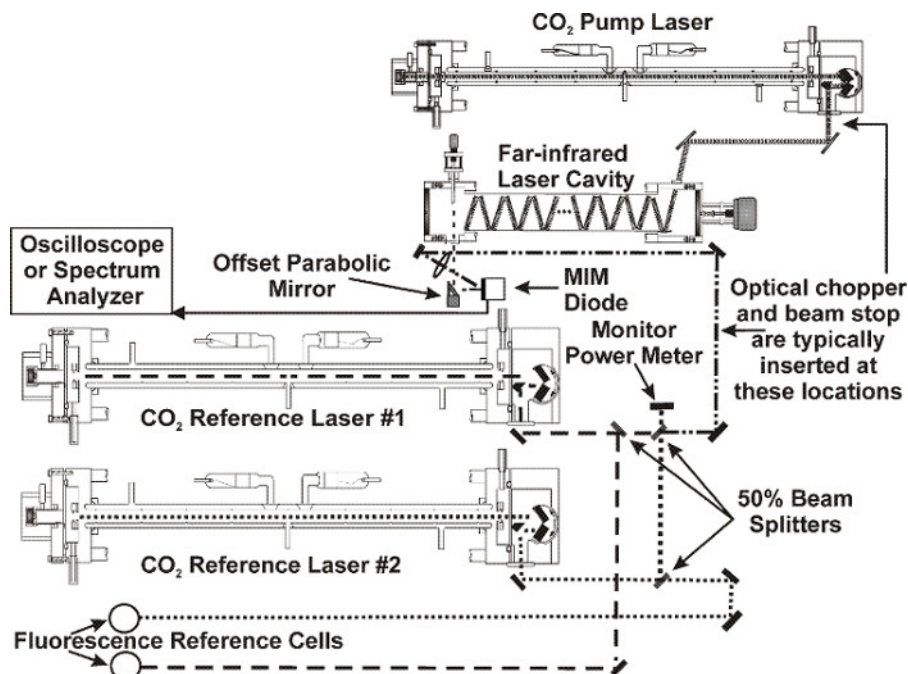
Figure 2. Schematic diagram of the three-laser heterodyne frequency measurement system. The heterodyne system includes the optically pumped molecular laser utilizing a transverse pumping geometry and two additional carbon dioxide reference lasers. Not shown are the electronic systems used to monitor and stabilize the radiation generated by each laser. © [2015] IEEE. Reprinted, with minor modifications and permission, from Ref. 27. Please click here to view a larger version of this figure.
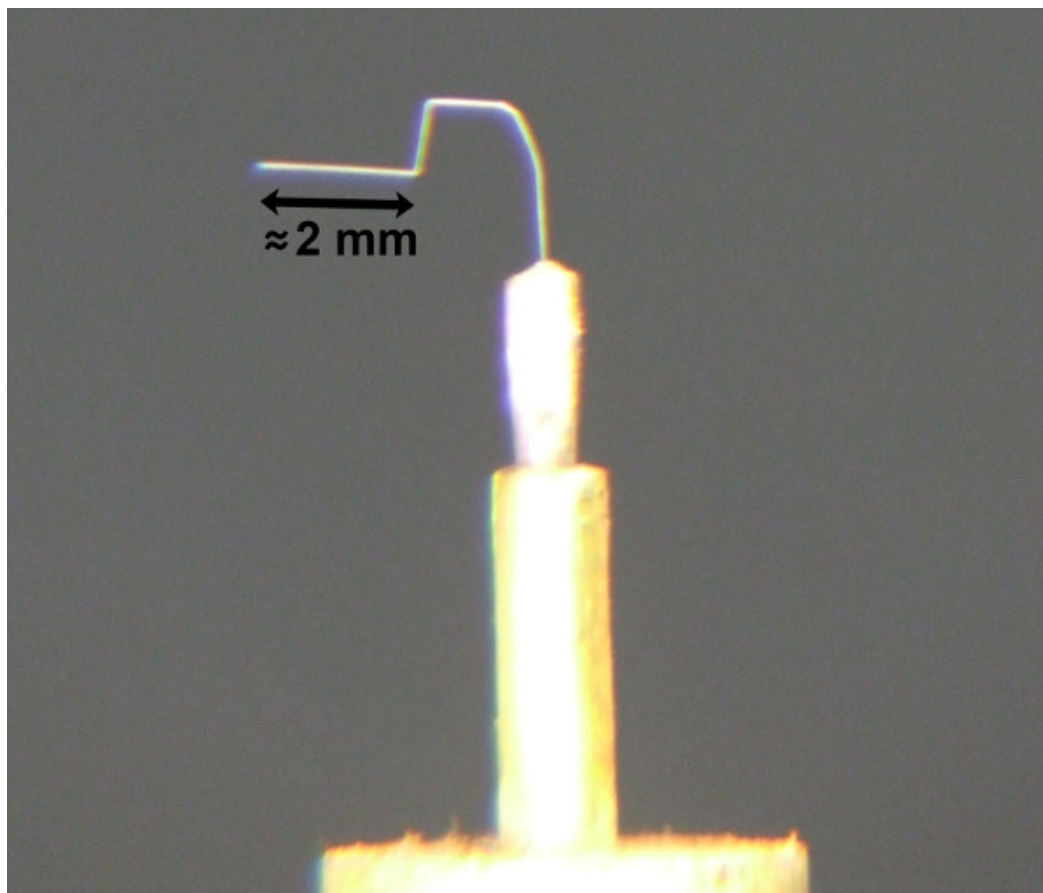

Figure 3. The Tungsten wire used in the MIM point contact diode detector as viewed through a magnifying lens. The length of the wire is approximately 2 mm. For best spring action, the angles in the bend should be near 90° and all lie in the same plane.
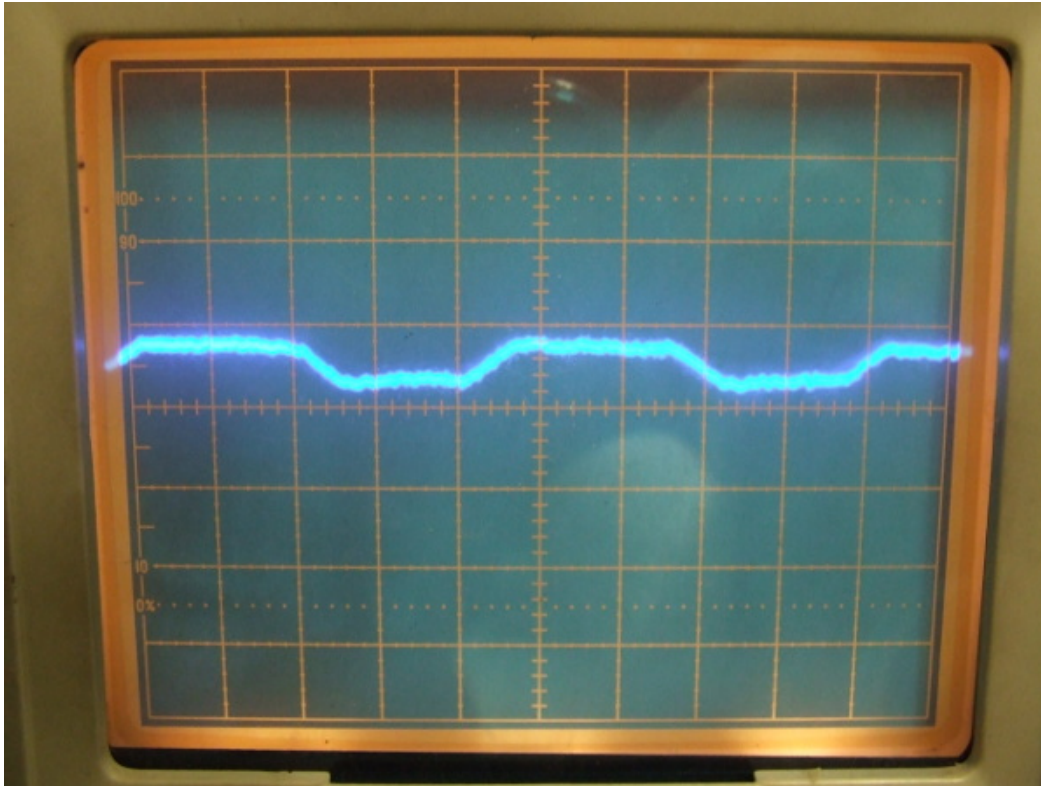
Figure 4. The waveform generated by the 274.8 µm laser emission of optically pumped CH_2F_2 using the 9*P*04 CO_2 pump laser as viewed on the oscilloscope display. The CO_2 pump radiation is modulated by an optical chopper operating at approximately 45 Hz. The resistance of the MIM diode detector is approximately 100 and the signal is approximately 6 µV (peak-to-peak). The oscilloscope display is set on 10 µV/division.
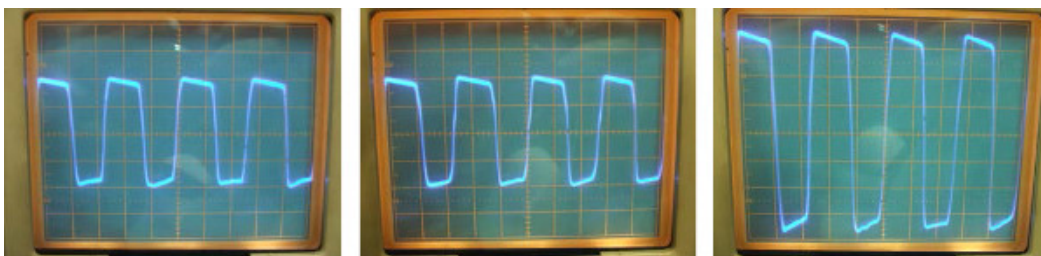

Figure 5. The left and middle photos show the output from each CO_2 reference laser, 9*R*16 and 9*P*34, respectively. The respective modulated signal on the oscilloscope is approximately 4 mV (peak-to-peak) for about 100 mW of power, as measured by the monitor power meter. The right photo shows the combined signal from both reference lasers to be approximately 7 mV (peak-to-peak) indicating the two reference signals are properly mixing on the MIM diode detector. The resistance of the MIM diode detector is approximately 100 Ω. The oscilloscope display in each photo is set on 1 mV/division. The CO_2 radiation is modulated by an optical chopper operating at approximately 70 Hz.
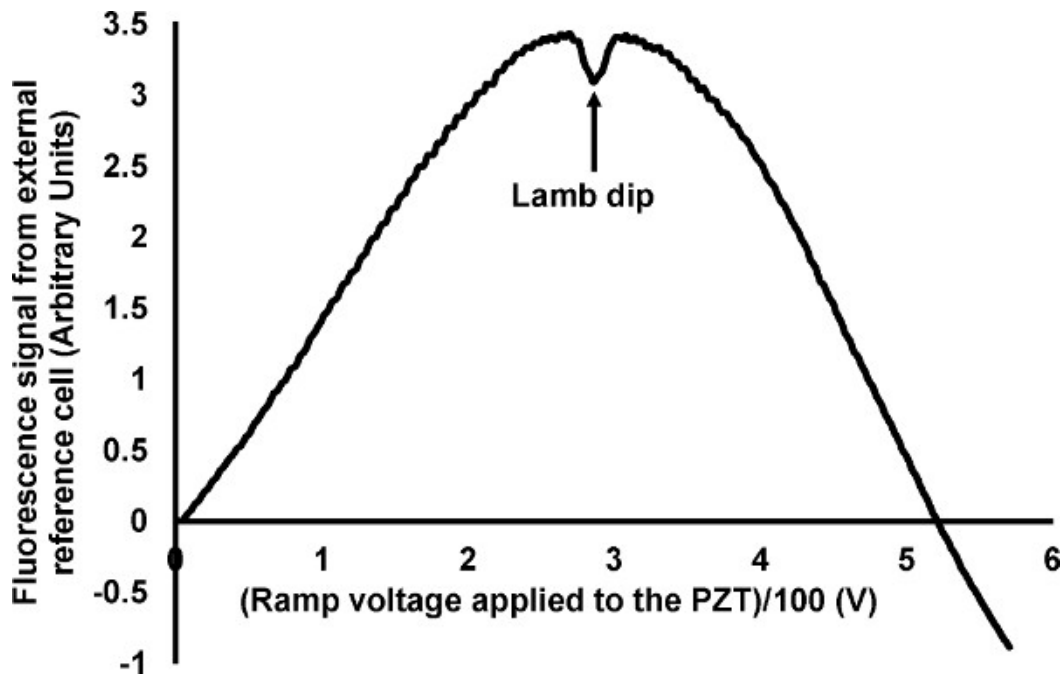
Figure 6. The saturated fluorescence signal in low pressure (6 Pa) CO_2 while using the $9R24$ CO_2 laser emission. This graph is obtained by modulating the CO_2 reference laser emission via an external chopper at 52 Hz while the voltage applied to the CO_2 reference laser's PZT is ramped from 0 to approximately 570 V in about 13 min. The lock-in amplifier is set to a 300 msec time constant and a 200 mV sensitivity. Please click here to view a larger version of this figure.
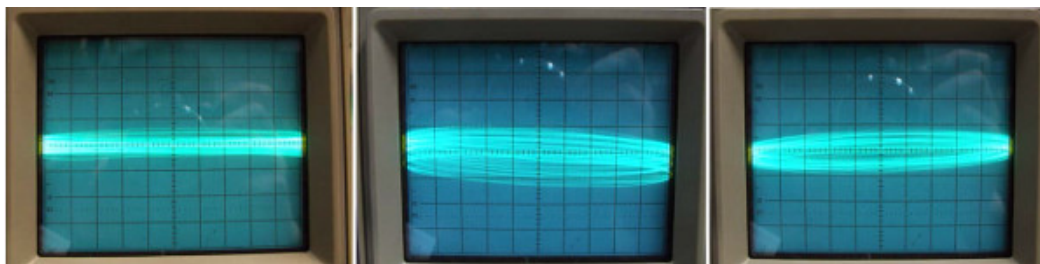
Figure 7. The saturated fluorescence signal in low pressure (6 Pa) CO_2 while using the $9R24$ CO_2 laser emission as viewed on an oscilloscope. The left photo indicates the oscilloscope display when the PZT voltage is away from the center of the Lamb dip, approximately 80 V in this photo. The middle and right photos indicate the oscilloscope display when the PZT voltage is either immediately to the left or right of the center of the Lamb dip, approximately 278 and 295 V respectively in these photos. Please click here to view a larger version of this figure.
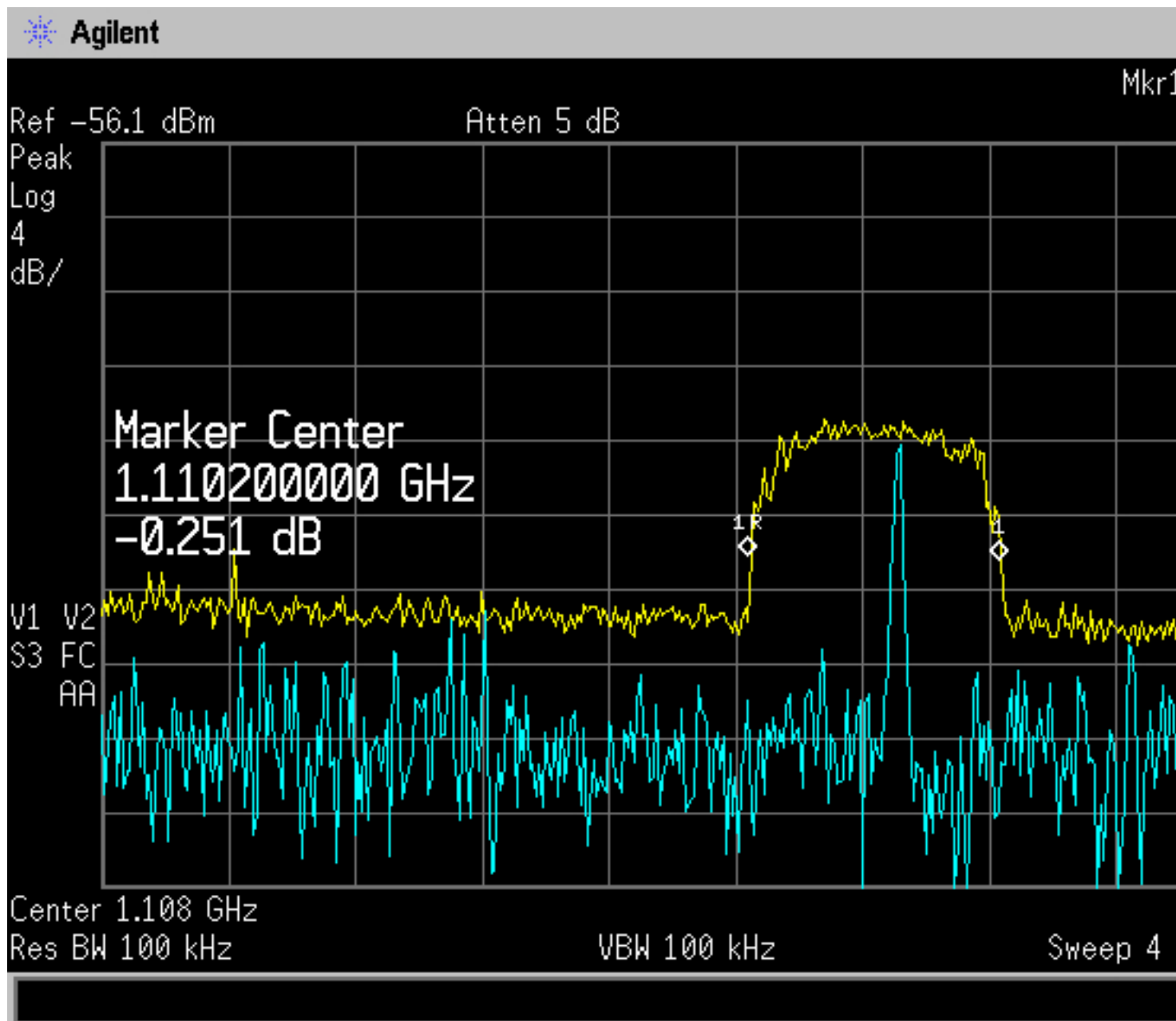
Figure 8. The beat signal between the 235.5 μm laser emission of optically pumped CH$_2$F$_2$ using the 9P04 CO$_2$ pump laser and the 9R16 and 9P34 CO$_2$ reference lasers. A span of approximately 25 MHz is typically used. The majority of beat signals are observed within ± 5 GHz. However, there are certain frequency regions within these search parameters that have a low signal-to-noise. Therefore, using a slightly larger search region has sometimes been helpful.
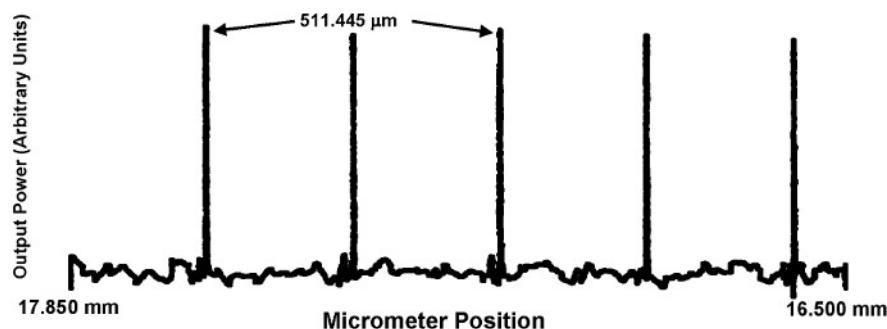
Figure 9. Portion of a typical laser resonator interferogram (or cavity scan) consisting of a set of discrete peaks that correspond to the resonator's modes, separated by regions where no lasing occurs. This scan shows the 511.445 µm laser emission generated by optically pumped CH_2F_2 using the $9R28$ CO_2 pump. A decrease in the micrometer position corresponds to a decrease in the length (mirror-to-mirror separation) of the far-infrared laser cavity. The MIM diode detected a 20 µV peak-to-peak maximum signal generated by this far-infrared laser emission. The output from the detector was recorded using a lock-in amplifier, set on a 300 msec time constant and 20 µV sensitivity, interfaced to a computer. Please click here to view a larger version of this figure.

CO_2 Reference Laser 1 [CO₂ (I)]		CO_2 Reference Laser 2 [CO₂ (II)]		|CO_2 Difference Frequency|	Predicted Beat Frequency
CO_2 laser emission	Frequency (MHz)	CO_2 laser emission	Frequency (MHz)	(MHz)	(MHz)
$10P\,44$	27 605 762.583	$10R\,02$	28 877 902.438	1 272 139.855	864
$10P\,34$	27 910 720.793	$10R\,16$	29 178 455.676	1 267 734.883	5269
$10P\,30$	28 027 431.871	$10R\,22$	29 296 136.369	1 268 704.498	4300
$10P\,20$	28 306 224.889	$10R\,38$	29 576 545.120	1 270 320.231	2684
$9P\,46$	30 610 516.143	$10R\,24$	29 333 861.159	1 276 654.984	−3651
$9P\,44$	30 674 445.772	$10R\,28$	29 407 038.249	1 267 407.523	5597
$9P\,38$	30 861 897.515	$9R\,10$	32 134 266.892	1 272 369.377	635
$9P\,34$	30 983 190.753	$9R\,16$	32 257 303.338	1 274 112.585	−1109
$9P\,30$	31 101 492.183	$9R\,22$	32 373 156.204	1 271 664.021	1340
$9P\,24$	31 273 247.148	$9R\,32$	32 550 429.164	1 277 182.015	−4178
$9P\,18$	31 438 060.175	$9R\,42$	32 708 262.438	1 270 202.264	2802
$9P\,16$	31 491 437.387	$9R\,46$	32 766 062.847	1 274 625.460	−1621
$9P\,14$	31 544 028.877	$9R\,50$	32 820 872.445	1 276 843.568	−3839

Table 1: Sets of CO_2 reference lasers whose difference frequency is near the calculated frequency for the 235.5 µm laser emission from optically pumped CH_2F_2 when excited using the $9P04$ CO_2 laser emission.

CO_2 (I)	$v_{CO2(I)}$ (MHz)	CO_2 (II)	$v_{CO2(II)}$ (MHz)	$\|v_{CO2(I)} - v_{CO2(II)}\|$ (MHz)	$\|v_{beat}\|$ (MHz)	Observation[a]	v_{FIR} (MHz)
9R 10	32 134 266.892	9P 38	30 861 897.515	1 272 369.377	633.15	increase	1 273 002.727
9R 10	32 134 266.892	9P 38	30 861 897.515	1 272 369.377	633.18		1 273 002.557
9R 10	32 134 266.892	9P 38	30 861 897.515	1 272 369.377	633.10		1 273 002.477
9R 10	32 134 266.892	9P 38	30 861 897.515	1 272 369.377	633.05	increase	1 273 002.427
9R 10	32 134 266.892	9P 38	30 861 897.515	1 272 369.377	633.18	increase	1 273 002.557
9R 10	32 134 266.892	9P 38	30 861 897.515	1 272 369.377	633.20		1 273 002.577
9R 10	32 134 266.892	9P 38	30 861 897.515	1 272 369.377	633.15	increase	1 273 002.527
9R 10	32 134 266.892	9P 38	30 861 897.515	1 272 369.377	633.05		1 273 002.427
9R 16	32 257 303.338	9P 34	30 983 190.753	1 274 112.585	1110.20	decrease	1 273 002.385
9R 16	32 257 303.338	9P 34	30 983 190.753	1 274 112.585	1110.05	decrease	1 273 002.535
9R 16	32 257 303.338	9P 34	30 983 190.753	1 274 112.585	1110.28		1 273 002.305
9R 16	32 257 303.338	9P 34	30 983 190.753	1 274 112.585	1110.00	decrease	1 273 002.585
9R 16	32 257 303.338	9P 34	30 983 190.753	1 274 112.585	1110.20		1 273 002.385
9R 16	32 257 303.338	9P 34	30 983 190.753	1 274 112.585	1109.98	decrease	1 273 002.605
			Average ± Standard Deviation				1 273 002.5 ± 0.1

[a] As outlined in step 3.4.5, this observation describes what happens to the beat frequency as the far-infrared laser frequency is slightly increased.

Table 2: Measured beat frequencies for the 235.5 μm laser emission from optically pumped CH_2F_2 when excited using the 9P04 CO_2 laser emission. Two sets of CO_2 reference lasers are used to generate the known difference frequency ($\|v_{CO2(I)} - v_{CO2(II)}\|$).

CO_2 Pump Laser	Wavelength (μm)	Frequency (MHz)	Wavenumber (cm^{-1})	Reference
9R 48	335.939	892 400.5 ± 0.5	29.7673	New[a]
9R 36	652.532	459 429.7 ± 0.3	15.3249	[15]
9P 04	235.500	1 273 002.5 ± 0.7	42.4628	New[b]
	274.831	1 090 825.7 ± 0.6	36.3860	[15]
	416.753	719 353.5 ± 0.5	23.9950	New[c]
	439.578	682 000.7 ± 0.5	22.7491	[15]
	835.476	358 828.3 ± 0.4	11.9692	[15]
9P 06	774.583	387 037.4 ± 0.4	12.9102	[15]

[a] Observed in the perpendicular polarization with an optimal operating pressure of 10 Pa.

[b] Observed in the parallel polarization with an optimal operating pressure of 8.7 Pa.

[c] Observed in both polarizations with an optimal operating pressure of 9.3 Pa.

Table 3: New far-infrared laser frequencies from optically pumped CH_2F_2.

CO_2 pump laser	The continuous wave CO_2 pump laser is 1.5 m long and uses a 151 line/mm grating that provides approximately 3% output coupling in the zeroth order. Infrared laser radiation is achieved on the 9R 50, 9P 54, 10R 52, and 10P 58 lines of the 9 and 10 micron branches with powers varying from about 2 to 18 W. The PZT is attached to the CO_2 pump laser's end mirror and is electrically isolated from the remainder of the laser cavity. The laser is home-made, constructed at the National Institute of Standards and Technology (NIST)-Boulder facility under the supervision and following the design of Dr. Ken Evenson.
Far-infrared laser	The far-infrared laser cavity has a 0.45 m long internally polished copper tube connected to two aluminum blocks by four Invar rods for thermal stability. The copper tube has a 0.051 m inner diameter and the far-infrared laser cavity uses two 1.2 m radius-of-curvature, gold-coated mirrors with a mirror-to-mirror separation that varies between 0.49 to 0.52 m. The calibrated micrometer is connected to the moveable end mirror. Far-infrared laser radiation is coupled out of the cavity by an adjustable 45° output coupler, approximately 1.05 cm in diameter, and through either a Teflon or polypropylene window. The laser is home-made, assembled at Central Washington University (CWU) with parts machined at CWU and the NIST-Boulder facility.
CO_2 reference lasers	The CO_2 reference lasers are 1.5 m long and generate lines out to 9R 48, 9P 48, 10R 48, and 10P 38 with powers up to several Watts. The lasers are home-made, constructed at the NIST-Boulder facility under the supervision and following the design of Dr. Ken Evenson.
CO_2 laser gas mixture and electrical power supply	CO_2 laser radiation is achieved using a Helium:Nitrogen:Carbon Dioxide (He:N_2:CO_2) gas mixture of 78%:12%:10% that is excited by a high voltage DC power supply. A Glassman KL series power supply provides approximately −7.5 kV across each cathode and ground delivering approximately 20 mA of current through each cathode. The remainder of the voltage, approximately −5.5 kV, is dropped across a set of ballast resistors (Ohmite 100 kW, 225 W resistors, model number L225J100K). Connection from the ballast resistors to the CO_2 laser cathodes were made using a CII Technologies HV relay, SPDT, model H-17.
Reference frequency stabilization system	The 4.3 µm fluorescence is monitored by an Indium Antimonide (InSb) liquid nitrogen cooled detector (Judson Infrared Inc, model J10D). The signal is amplified (Princeton Applied Research, model PAR 113 pre-amp) after passing through impedence matched transformers. The amplified signal is sent to a NIST custom built lock-in servo. This lock-in provides a voltage to control the PZT, via a NIST custom built high voltage (HV) amplifier, of the respective reference CO_2 laser in order to keep the laser locked to the Lamb dip in the fluorescence signal from the external, low pressure reference cell. The reference frequency is typically 731 Hz with an approximate 3 V peak-to-peak modulation voltage. The output of the pre-amp is monitored using an oscilloscope (Tektronix, model 2235A) to provide a visual indication about whether the reference laser is locked to the center of the Lamb dip. The custom built NIST Asymmetric HV Amp is powered by a Fluke, model 412B, high voltage power supply.
CO_2 laser tube and reference cell	The Pyrex-glass CO_2 laser tube has an inner ribbed tube surrounded by a water-cooled jacket. The inner and outer diameters of the glass tube are approximately 15 and 30 mm, respectively. By introducing glass ribs into the laser cavity many wall-bounce modes are eliminated, thereby forcing an open-structure mode and increasing the effective resolution of the grating[56]. The CO_2 laser tubes and the low pressure reference cells were made at Allen Scientific Glass (Boulder, CO) following the design of Dr. Ken Evenson.

Supplemental Table A: Technical details of the experimental system including some relevant commercial components.

Discussion

There are several critical steps within the protocol that require some additional discussion. When measuring the far-infrared laser wavelength, as outlined in step 2.5.3, it is important to ensure the same mode of the far-infrared laser emission is being used. Multiple modes of a far-infrared laser wavelength (*i.e.*, TEM_{00}, TEM_{01}, etc.) can be generated within the laser cavity and thus it is important to identify the appropriate adjacent cavity modes being used to measure the wavelength[13,29,41]. To assist in eliminating higher order modes, irises are included within each laser cavity. When accurately measuring a far-infrared laser frequency, it is imperative the lasers, particularly the CO_2 reference lasers, operate in their fundamental (TEM_{00}) mode. Irises are also used to ensure the pattern traced out by the far-infrared laser on the spectrum analyzer is symmetric. For situations where multiple far-infrared laser wavelengths are generated by a particular CO_2 pump line, as in the case of 9*P*04, a set of absorbing filters, calibrated with wavelength, are used to assist in distinguishing far-infrared laser wavelengths. They can also be used to attenuate any scattered CO_2 laser radiation exiting the far-infrared laser cavity.

Section 2.4 describes the generation of far-infrared laser radiation. Over numerous investigations, we have found that multiple distinct wavelengths could be generated by the same CO_2 pump laser set at slightly different offset frequencies. For example, the 9*P*04 CO_2 pump laser is capable of generating the 289.5 and 724.9 µm wavelengths of CH_2F_2 at one pump frequency while the remaining wavelengths measured during this investigation were generated using a slightly different frequency from the 9*P*04 CO_2 pump laser. This is accomplished by changing the voltage applied to the PZT that tunes the frequency of the CO_2 pump laser through its broadened gain curve (approximately ± 45 MHz from its center frequency in this experiment). Although not specifically addressed in section 2.4, we believe this is a noteworthy feature in searching for far-infrared laser radiation.

For situations where multiple far-infrared laser emissions are generated by the same CO_2 pump laser line at the same offset frequency, a laser resonator interferogram (or cavity scan) can be performed to assist in identifying the different far-infrared laser emissions being generated. **Figure 9** illustrates a portion of a typical laser resonator interferogram, with the output power plotted as a function of decreasing far-infrared laser cavity length[42–45].

As outlined in section 3.4, two distinct sets of CO_2 reference lasers are used to measure the far-infrared laser frequency. This helps eliminate the uncertainty about whether the beat frequency is above or below the difference frequency generated between the CO_2 reference lasers. Along with providing a way to independently verify the far-infrared laser frequency, it has been particularly useful when working with weak beat signals where observing the slight shift in the beat frequency as the far-infrared laser frequency increases can be challenging.

The MIM diode detector is an essential component to this experimental system due to its high speed, sensitivity, and broad spectral coverage[23,24]. However, there are some limitations to the MIM diode detector that include mechanical instability, susceptibility to electromagnetic disturbances, poor reproducibility, and a limit to the maximum power it is capable of detecting while maintaining its sensitivity. While measuring far-infrared laser frequencies, the sensitivity of the MIM diode detector was found to decrease rapidly over time if the power from each CO_2 reference laser exceeded 150 mW.

Beyond the MIM diode detector, the main limitation to the present technique is the stability of the far-infrared laser[4,31,46]. A limitation in the experimental system's current configuration is the inability to measure the offset frequency of the CO_2 pump laser. As mentioned, the offset frequency is defined as the difference between the frequency used by the CO_2 pump laser to generate the far-infrared laser emission and the CO_2 pump laser's center frequency. Thus it represents the difference between the absorption frequency of the far-infrared laser medium and the center frequency of the CO_2 pump laser. Typically, the offset frequency is readily measured using any CO_2 laser radiation that is inadvertently scattered out of the far-infrared laser cavity. In our current configuration however, very little CO_2 laser radiation is available for such a measurement. Other methods of measuring the offset frequency could be incorporated into future iterations of the project. This includes using additional beam splitters and mirrors to couple a portion of the pump radiation to the MIM diode detector. The measurement of an offset frequency is beneficial when assigning spectroscopic transitions to the far-infrared laser emission[25,34].

Far-infrared laser frequencies have also been measured by heterodyning two optically pumped far-infrared lasers and a microwave source on a MIM diode detector whereby the frequency of one of the two far-infrared lasers is known and is used as the reference frequency[47]. The use of far-infrared frequencies with greater accuracy is possible using other techniques, such as with THz frequency-comb synthesis similar to those discussed in Refs. 48-54. Measuring laser frequencies expands the role of optically pumped molecular lasers in THz applications from THz imaging[55], its role as a source of THz radiation for high-resolution spectroscopy[13,20], and in assisting with the analysis of the complex spectra associated with its lasing medium[19,34,37].

Disclosures

Certain commercial equipment is identified in this paper to foster understanding. Such identification does not imply recommendation or endorsement by the authors, nor does it imply that the equipment identified is necessarily the best available for the purpose.

Acknowledgements

References

1. Hocker, L.O., Javan, A., Ramachandra Rao, D., Frenkel, L., Sullivan, T. Absolute frequency measurement and spectroscopy of gas laser transitions in the far infrared. *Appl. Phys. Lett.* **10** (5), 147-149 (1967).

2. Wells, J.S., Evenson, K.M., Day, G.W., Halford, D. Role of infrared frequency synthesis in metrology. *Proc. IEEE.* **60** (5), 621-623 (1972).

3. Whitford, B.G., Siemsen, K.J., Riccius, H.D., Baird, K.A. New frequency measurements and techniques in the 30-THz region. *IEEE Trans. Instrum. Meas.* **23** (4), 535-539 (1974).

4. Petersen, F.R., *et al.* Far infrared frequency synthesis with stabilized CO_2 lasers: Accurate measurements of the water vapor and methyl alcohol laser frequencies. *IEEE J. Quantum Elect.* **11** (10), 838-843 (1975).

5. Uranga, C., Connell, C., Borstad, G.M., Zink, L.R., Jackson, M. Discovery and frequency measurement of short-wavelength far-infrared laser emissions from optically pumped $^{13}CD_3OH$ and CHD_2OH. *Appl. Phys. B.* **88** (4), 503-505 (2007).

6. Jackson, M., Milne, J.A., Zink, L.R. Measurement of optically pumped $CH_3^{18}OH$ laser frequencies between 3 and 9 THz. *IEEE J. Quantum Elect.* **47** (3), 386-389 (2011).

7. Evenson, K.M., *et al.* Optically pumped FIR lasers: Frequency and power measurements and laser magnetic resonance spectroscopy. *IEEE J. Quantum Elect.* **13** (6), 442-444 (1977).

8. Evenson, K.M., Jennings, D.A., Petersen, F.R. Tunable far-infrared spectroscopy. *Appl. Phys. Lett.* **44** (6), 576-577 (1984).

9. Evenson, K.M., *et al.* Speed of light from direct frequency and wavelength measurements of the methane-stabilized laser. *Phys. Rev. Lett.* **29** (19), 1346-1349 (1972).

10. Comptes Rendus des Séances de la 17e Conférence Générale des Poids et Mesures, BIPM, *Resolution 1*, 97-98, Sevres, France (1983).

11. Giacomo, P. News from the BIPM. *Metrol.* **20** (1), 25-30 (1984).

12. Chang, T.Y., Bridges, T.J. Laser action at 452, 496 and 541 µm in optically pumped CH_3F. *Opt. Commun.* **1** (9), 423-426 (1970).

13. Douglas, N.G. *Millimetre and Submillimetre Wavelength Lasers: A Handbook of CW Measurements. Springer Series in Optical Sciences.* Volume **61**, Walther, H., ed., Springer-Verlag (1989).

14. Zerbetto, S.C., Vasconcellos, E.C.C., Zink, L.R., Evenson K.M. $^{12}CH_2F_2$ and $^{13}CH_2F_2$ far-infrared lasers: New lines and frequency measurements. *Int. J. Infrared Millim. Waves.* **18** (12), 2301-2306 (1997).

15. Jackson, M., Alves, H., Holman, R., Minton, R., Zink, L.R. New cw optically pumped far-infrared laser emissions generated with a transverse or 'zig-zag' pumping geometry. *J. Infrared, Millim., Terahertz Waves.* **35** (3), 282-287 (2014).

16. Danielewicz, E.J. The optically pumped difluoromethane far-infrared laser. *Reviews of Infrared and Millimeter Waves.* Volume **2**, Button, K.J., Inguscio, M., Strumia, F., eds., Plenum, 223-250 (1983).

17. Deroche, J.-C., Benichou, E.-K., Guelachvili, G., Demaison, J. Assignments of submillimeter emissions in difluoromethane pumped by $^{12}C^{18}O_2$ and $^{12}C^{18}O_2$ lasers. *Int. J. Infrared Millim. Waves.* **7** (10), 1653-1675 (1986).

18. Jackson, M., Zink, L.R., McCarthy, M.C., Perez, L., Brown, J.M. The far-infrared and microwave spectra of the CH radical in the v = 1 level of the $X^2\Pi$ state. *J. Mol. Spectrosc.* **247** (2), 128-139 (2008).

19. Zhao, S., Lees, R.M. $CH_3^{18}OH$: Assignment of FIR laser lines optically pumped in the in-plane CH_3-rocking band. *J. Mol. Spectrosc.* **168** (1), 67-81 (1994).

20. Evenson, K.M., Saykally, R.J., Jennings, D.A., Curl, R.F., Brown, J.M. Far infrared laser magnetic resonance. *Chemical and Biochemical Applications of Lasers.* Academic Press. **5**, 95-138 (1980).

21. Hocker, L.O., Sokoloff, D.R., Daneu, V., Szoke, A., Javan, A. Frequency mixing in the infrared and far-infrared using a metal-to-metal point contact diode. *Appl. Phys. Lett.* **12** (12), 401-402 (1968).

22. Daneu, V., Sokoloff, D., Sanchez, A., Javan, A. Extension of laser harmonic-frequency mixing techniques into the 9 µ region with an infrared metal-metal point-contact diode. *Appl. Phys. Lett.* **15** (12), 398-400 (1969).

23. Jennings, D.A., Evenson, K.M., Knight, D.J.E. Optical Frequency Measurements. *Proc. IEEE.* **74** (1), 168-179 (1986).

24. Zink, L.R. *Highly accurate molecular constants for CO, HF, HCl, OH, NaH, MgH, and O_2: Rotational transition frequencies measured with tunable far infrared radiation.* PhD Thesis. University of Colorado (1986).

25. Xu, L.-H., *et al.* Methanol and the optically pumped far-infrared laser. *IEEE J. Quantum Elect.* **32** (3), 392-399 (1996).

26. Jackson, M., Zink, L.R., Garrod, T.J., Petersen, S., Stokes, A., Theisen, M. The generation and frequency measurement of short-wavelength far-infrared laser emissions. *IEEE J. Quantum Elect.* **41** (12), 1528-1532 (2005).

27. Jackson, M., Smith, M., Gerke, C., Barajas, J.M. Measurement of far-infrared laser frequencies from methanol isotopologues. *IEEE J. Quantum Elect.* **51** (4), Article No. 1500105 (2015).

28. Freed, C., Javan, A. Standing-wave saturation resonances in the CO_2 10.6 µ transitions observed in a low-pressure room-temperature absorber gas. *Appl. Phys. Lett.* **17** (2), 53-56 (1970).

29. DeShano, B., Olivier, K., Cain, B., Zink, L.R., Jackson, M. Using guide wavelengths to assess far-infrared laser emissions. *J. Infrared, Millim., Terahertz Waves.* **36** (1), 13-30 (2015).

30. Jackson, M., Nichols, A.J., Womack, D.R., Zink, L.R. First laser action observed from optically pumped $CH_3^{17}OH$. *IEEE J. Quantum Elect.* **48** (3), 303-306 (2012).

31. Inguscio, M., Moruzzi, G., Evenson, K.M., Jennings, D.A. A review of frequency measurements of optically pumped lasers from 0.1 to 8 THz. *J. Appl. Phys.* **60** (12), R161-R191 (1986).

32. Pereira, D., *et al.* A review of optically pumped far-infrared laser lines from methanol isotopes. *Int. J. Infrared Millim. Waves.* **15** (1), 1-44 (1994).

33. Zerbetto, S.C., Vasconcellos, E.C.C. Far infrared laser lines produced by methanol and its isotopic species: A review. *Int. J. Infrared Millim. Waves.* **15** (5), 889-933 (1994).

34. Moruzzi, G., Winnewisser, B.P., Winnewisser, M., Mukhopadhyay, I., Strumia, F. *Microwave, Infrared and Laser Transitions of Methanol: Atlas of Assigned Lines from 0 to 1258 cm^{-1}.* CRC Press, FL (1995).

35. Weber, M.J. ed., *Handbook of Laser Wavelengths.* CRC Press, FL (1999).

36. De Michele, A., *et al.* FIR laser lines from CH_3OD: A review. *Int. J. Infrared Millim. Waves.* **25** (5), 725-734 (2004).

37. De Michele, A., Carelli, G., Moruzzi, G., Moretti, A. Hydrazine far-infrared laser lines and assignments: a review. *J. Opt. Soc. Am. B.* **22** (7), 1461-1470 (2005).

38. Moraes, J.C.S. *et al.* Experimental investigation of $^{13}CD_3OH$ infrared transitions by means of optoacoustic spectroscopy. *Int. J. Infrared Millim. Waves.* **13** (11), 1801-1823 (1992).

39. Viscovini, R.C., Scalabrin, A., Pereira, D. Infrared optoacoustic spectroscopy of $^{13}CD_3OD$ around the 10R and 10P CO_2 laser lines. *Int. J. Infrared Millim. Waves.* **17** (11), 1821-1838 (1996).

40. Maki, A.G., Chou, C.C., Evenson, K.M., Zink, L.R., Shy, J.T. Improved molecular constants and frequencies for the CO_2 laser from new high-J regular and hot-band frequency measurements. *J. Mol. Spectrosc.* **167** (1), 211-224 (1994).

41. Douglas, N.G., Krug, P.A. CW laser action in ethyl chloride. *IEEE J. Quantum Elect.* **18** (10), 1409-1410 (1982).

42. Schwaller, P., Steffen, H., Moser, J.F., Kneubühl, F.K. Interferometry of resonator modes in submillimeter wave lasers. *Appl. Opt.* **6** (5), 827-829 (1967).
43. Steffen, H., Kneubühl, F.K. Resonator interferometry of pulsed submillimeter-wave lasers. *IEEE J. Quantum Elect.* **4** (12), 992-1008 (1968).
44. Whitbourn, L.B., Macfarlane, J.C., Stimson, P.A., James, B.W., Falconer, I.S. An experimental study of a cw optically pumped far infrared formic acid vapour laser. *Infrared Phys.* **28** (1), 7-20 (1988).
45. Belland, P., Véron, D., Whitbourn, L.B. Mode study, beam characteristics and output power of a cw 337 μm HCN waveguide laser. *J. Phys. D: Appl. Phys.* **8** (18), 2113-2122 (1975).
46. Inguscio, M., Ioli, N., Moretti, A., Strumia, F., D'Amato, F. Heterodyne of optically pumped FIR molecular lasers and direct frequency measurement of new lines. *Appl. Phys. B.* **40** (3), 165-169 (1986).
47. Carelli, G., *et al.* $CH_3^{18}OH$: FIR laser line frequency measurements and assignments. *Infrared Phys. Technol.* **35** (6), 743-755 (1994).
48. Pearson, J.C., Müller, H.S.P., Pickett, H.M., Cohen, E.A., Drouin, B.J. Introduction to submillimeter, millimeter and microwave spectral line catalog. *J. Quant. Spectrosc. Radiat. Transf.* **111** (11), 1614-1616 (2010).
49. Ehasz, E.J., Goyette, T.M., Giles, R.H., Nixon, W.E. High-resolution frequency measurements of far-infrared laser lines. *IEEE J. Quantum Elect.* **46** (4), 474-477 (2010).
50. Pearson, J.C., Drouin, B.J., Yu, S., Gupta, H. Microwave spectroscopy of methanol between 2.48 and 2.77 THz, *J. Opt. Soc. Am. B.* **28** (10), 2549-2577 (2011).
51. Consolino, L., *et al.* Phase-locking to a free-space terahertz comb for metrological-grade terahertz lasers. *Nat. Commun.* **3**, Article No. 1040 (2012).
52. Bartalini, S., *et al.* Frequency-comb-assisted terahertz quantum cascade laser spectroscopy. *Phys. Rev. X.* **4** (2), 021006 (2014).
53. Finneran, I.A., Good, J.T., Holland, D.B., Carroll, P.B., Allodi, M.A., Blake, G.A. Decade-spanning high-precision terahertz frequency comb. *Phys. Rev. Lett.* **114** (16), Article No. 163902 (2015).
54. De Natale, P., *et al. Quantum cascade laser THz metrology. Proc. SPIE.* **9370**, *Quantum Sensing and Nanophotonic Devices XII*, 93701D (2015).
55. Dickinson, J.C., Goyette, T.M., Waldman, J. High resolution imaging using 325 GHz and 1.5 THz transceivers. *15th International Symposium on Space Terahertz Technology Proceedings.* 373-380 (2004).
56. Vasconcellos, E.C.C., Zerbetto, S.C., Holecek, J.C., Evenson, K.M. Short-wavelength far-infrared laser cavity yielding new lines in methanol. *Opt. Lett.* **20** (12), 1392-1393 (1995).